

Conf-9505192--3

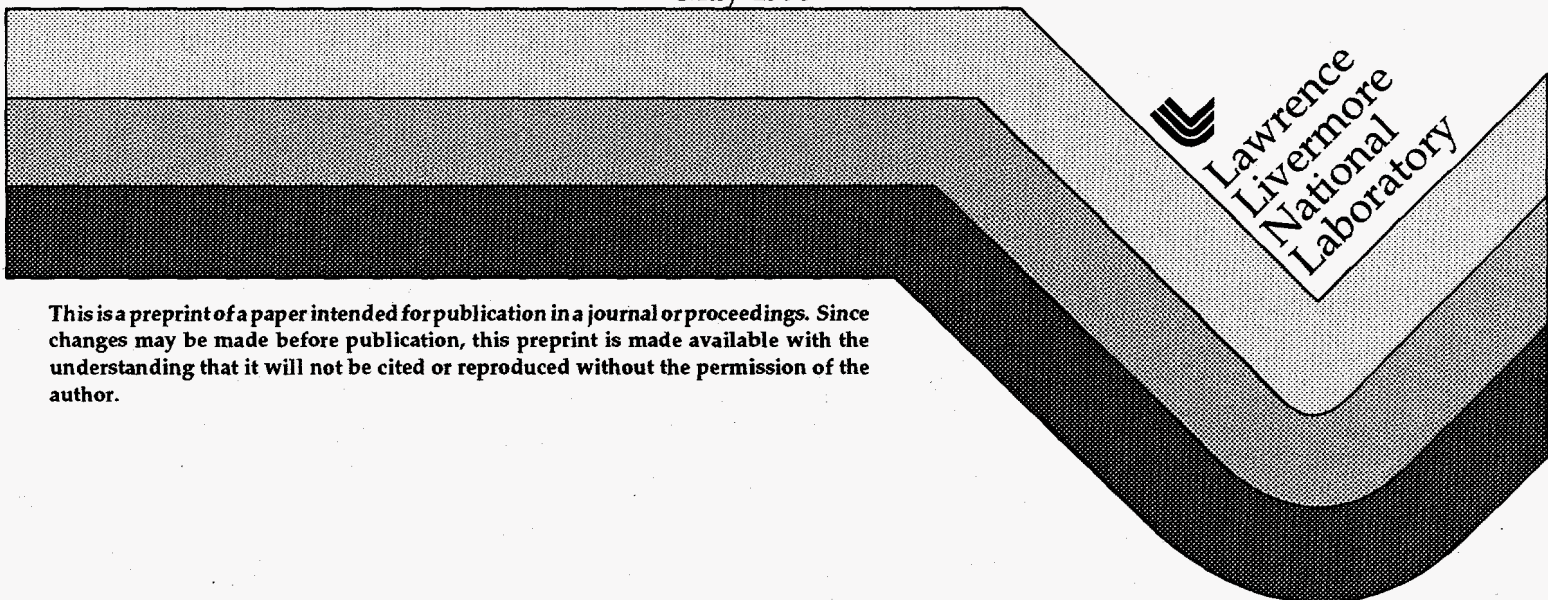
UCRL-JC-119571
PREPRINT

Molecular Dynamics Modeling of Ultrathin Amorphous Carbon Films

J.N. Glosli
J. Belak
M.R. Philpott

This paper was prepared for submittal to the
Fourth International Symposium on Diamond Material
Reno, Nevada
May 21-26, 1995

May 1995



This is a preprint of a paper intended for publication in a journal or proceedings. Since changes may be made before publication, this preprint is made available with the understanding that it will not be cited or reproduced without the permission of the author.

DISCLAIMER

This document was prepared as an account of work sponsored by an agency of the United States Government. Neither the United States Government nor the University of California nor any of their employees, makes any warranty, express or implied, or assumes any legal liability or responsibility for the accuracy, completeness, or usefulness of any information, apparatus, product, or process disclosed, or represents that its use would not infringe privately owned rights. Reference herein to any specific commercial product, process, or service by trade name, trademark, manufacturer, or otherwise, does not necessarily constitute or imply its endorsement, recommendation, or favoring by the United States Government or the University of California. The views and opinions of authors expressed herein do not necessarily state or reflect those of the United States Government or the University of California, and shall not be used for advertising or product endorsement purposes.

DISCLAIMER

Portions of this document may be illegible in electronic image products. Images are produced from the best available original document.

MOLECULAR DYNAMICS MODELING OF ULTRATHIN AMORPHOUS CARBON FILMS

James N. Glosli*, James Belak* and
Michael R. Philpott†

*Lawrence Livermore National Laboratory
University of California, Livermore, CA 94551

†IBM Research Division, Almaden Research Center
650 Harry Road, San Jose, CA 95120-6099

Amorphous carbon films about 20 nm thick are used by the computer industry as protective coatings on magnetic disks. The structure and function of this family of materials at the atomic level is poorly understood. The growth and properties of a:C and a:CH films 1 to 5 nm thick has been simulated using classical molecular dynamics and a bond-order potential with torsional terms. Studies of quenched melts that verify the ability of this potential to reproduce known features of extended structures of carbon in two and three dimensions are briefly described. In molecular dynamics calculations the incident species were neutral atoms C, or C and H with energies up to 100 eV. The stoichiometry, chemical bonding and distribution functions within the films were analyzed using IBM's Power Visualization System for different incident gas energies. Microscopic features such as multiple ring structures, including planar graphitic structures, were easily identified. Some preliminary studies of the nanotribology of the a:C films are described, including nano-indentation and sliding in contact with a rigid probe.

INTRODUCTION

In the computer information storage technology the surfaces of rigid disks in direct access storage devices are protected by a thin layer of amorphous carbon hydrogen a:CH (< 20 nm thick), on top of which is an even thinner layer of a perfluorinated polyether lubricant (< 3 nm). The purpose of the carbon overcoat (COC) is to protect the magnetic layer in which the information is encoded, from corrosion, abrasion, and impacts with asperities on the slider. The typical flying height and velocity of the slider are 50 to 75 nm and 1 to 40 ms⁻¹ respectively. These dimensions and speeds permit the application of molecular dynamics simulations¹ to model physical and chemical processes occurring inside this technologically very important slider-disk interface. Here we report on the growth, chemical composition, and physical structure of amorphous carbon a:C films with thickness's in the very small to small nanometer range. Some comments on the growth and properties of a:C-H films, and the tribology (friction, lubrication and

MASTER

DISTRIBUTION OF THIS DOCUMENT IS UNLIMITED DC

wear) of a:C films are also given. The immediate objective was to simulate films that have a composition in the range used on computer disks, and tribological tests like indentation and sliding, in order to compare with real COCs. These calculations contain novel features that make them of interest in connection with chemical vapor deposition, chemistry of nanomachining of covalent solids and energy dissipation processes². A brief account of this work at an earlier stage of progress has been published³.

The experimental characterization of non crystalline thin films is not particularly easy and it is no surprise that even after many years of study amorphous carbon films are still poorly understood. For this reason molecular dynamics simulations could turn out to be an important tool for understanding theoretically what is already known experimentally. Many of the early studies characterized the chemical bonding in the films using vibrational spectroscopy⁴⁻⁶. However the information obtained was not detailed because of the intrinsic disorder of the material. Recently pulsed NMR techniques have given more quantitative information on composition and bonding ratios in thick films⁷. Likewise the brightness of synchrotron sources in the x-ray region has made some measurement of radial distribution functions possible⁸ which can also be compared with neutron scattering⁹.

THE MOLECULAR DYNAMICS MODEL

In a typical classical molecular dynamics (MD) scheme the equations of classical mechanics are numerically integrated with time steps around 1 fs (10^{-15} seconds) for several million times steps. The forces are generated by differentiating a potential energy function. In the past the development of potentials associated with directed chemical bonds in organic materials was achieved assuming that they did not stretch to breaking point. These potentials are suitable for studying the conformations and vibrations of single molecules or polymers or assemblies of the same¹⁰. They are not useful in problems of the type described here, where chemical reactions occur during the growth of the carbon film or as a result of a tribological process. Instead we follow the idea of a bond order potential¹¹, extended in essential ways to strong covalently bonded systems like silicon and carbon by Tersoff¹²⁻¹⁴, and elaborated into a practical and useable form for carbon and carbon-hydrogen systems by Brenner¹⁵⁻¹⁷.

In Brenner's scheme the interatomic potentials allow incident neutral C and H atoms to bond to previously deposited atoms in ways that are determined by the bonding state of nearest and next nearest neighbors. These potentials have the advantage that they permit the making and breaking of bonds with the arrival of each new atom. The basic form of the potential is

$$E_{\text{bonds}} = \frac{1}{2} \sum_i E_i = \sum_i \sum_{j(\neq i)} [V_R(r_{ij}) - \bar{B}_{ij} V_A(r_{ij})].$$

where the labels i and j run over all atoms in the system. The V_R and V_A are repulsive and attractive Morse like potentials given by

$$V_R(r_{ij}) = f_{ij}(r_{ij}) D_{ij}^{(e)} \frac{S_{ij}}{(S_{ij} - 1)} e^{-\sqrt{2S_{ij}} \beta_{ij}(r - R_{ij}^{(e)})}$$

$$V_A(r_{ij}) = f_{ij}(r_{ij}) D_{ij}^{(e)} \frac{S_{ij}}{(S_{ij} - 1)} e^{-\sqrt{\frac{2}{S_{ij}}} \beta_{ij}(r - R_{ij}^{(e)})}$$

where the cut-off functions $f_{ij}(r)$ are chosen to be differentiable and to restrict the potential to nearest neighbours. If S_{ij} is set to 2 these functions revert to the usual Morse form. The two body Morse form describes what happens as the bond is stretched to breaking. The three (bond angle bends) and four (torsions) body terms are contained in the bond order function \bar{B}_{ij} . The interested reader is referred to the papers of Brenner^{15, 16} for full details. Only the salient features are given here.

$$\bar{B}_{ij} = \frac{1}{2}(B_{ij} + B_{ji}) + F_{ij}(N_i^{(t)}, N_j^{(t)}, N_{ij}^{conj}) + C_{ij}(N_i^{(t)}, N_j^{(t)}, N_{ij}^{conj}) T_{ij}$$

where

$$B_{ij} = (1 + H_{ij} + U_{ij})^{-\delta_i}$$

$$H_{ij} = H_{ij}(N_i^{(H)}, N_i^{(C)})$$

$$U_{ij} = \sum_{k(\neq i, j)} G_i(\theta_{ijk}) f_{ik}(r_{ik}) e^{\alpha_{ijk}[(r_{ij} - R_{ij}^{(e)}) - (r_{ik} - R_{ik}^{(e)})]}$$

$$T_{ij} = \sum_{kl(\neq i, j)} [1 - (\cos \phi_{ijkl})^2] f_{ik}(r_{ik}) f_{jl}(r_{jl})$$

In these formulas $G_i(\theta_{ijk})$ describes the three atom angle bends and $T_{ij}(\phi_{ijkl})$ the four atom torsions. In the dihedral torsion angle ϕ_{ijkl} the quadruples $ijkl$ assume that ij is the bond around which torsion occurs, and that bonds connect k to i and l to j . The symbols $N_i^{(C)}$, $N_i^{(H)}$, $N_i^{(t)}$, and N_{ij}^{conj} refer to functions which represent the number of carbon, hydrogen, total carbon and hydrogen and the number of conjugated pairs of carbon atoms. The cut-off functions $f_{ij}(r)$ are used to define the number functions N_i . The conjugation number function provides continuous values of N_{ij}^{conj} as bonds are created or destroyed. When $N_{ij}^{conj} = 1$ then the bond ij is not part of a conjugated system. When $N_{ij}^{conj} \geq 2$ the bond ij is part of a conjugated system and parameters fitted to conjugated bonds are used. The explicit form of $T_{ij}(\phi_{ijkl})$ used in the calculations reported here is similar to that used by Brenner¹⁷.

QUENCHED MELTS

As a test of the use of the Brenner potentials we have simulated the cooling of pure carbon melts of various densities. For the quench simulation we use periodic boundary conditions and constrain the volume to fix the density relative to diamond density ($\rho_D = 3.54$ grms/cc). The initial state was the well equilibrated liquid at 6000 K. System sizes from 64 to 8000 carbon atoms and quench rates from 5 to 40 K/ps were studied. Without the torsional term the system adopted unphysical bonding configurations when two sp^2 C atoms were directly bonded. The torsional term was included in all the calculations reported here. For a given density the pair distribution function was found to be relatively insensitive to quench rate and system size. The pair distribution curve was found to be similar to that in the tight binding MD simulations of Drabold et al¹⁸. In some of the quenches at densities around $0.5\rho_D$ we observed the formation of 2D graphitic layers of trigonally bonded sp^2 C atoms containing numerous defects, mostly in the form of five and seven membered rings with a few eight membered rings. The sheets tended to be planar across the entire simulation cell. In other quenches at similar densities we observed the formation of amorphous three dimensional networks with mostly trigonally bonded C atoms with five, six, seven and eight membered rings. At densities closer to ρ_D amorphous 3D carbon networks with high sp^3 bond content were formed, with many paired sp^2 C atoms. Based on their high sp^3 bond content these networks appear to model diamond-like carbon films quite well.

AMORPHOUS a:C FILMS

Amorphous a:C and a:CH films have been simulated for different growth conditions and with different feed stocks (C, H, C_2 , and benzene have all been tried). In the calculations reported here beams of neutral C or H atoms with predetermined kinetic energies (in the range 1 to 100 eV) impinged on a diamond (100) surface. The dynamics of the diamond substrate was governed by the Brenner potentials. As the a:C or a:CH film grew the diamond surface was buried and the film lost memory of its substrate. A great deal of effort was put into choosing a good thermostating scheme because of the large amount of energy released when an incident C atom bonded to the surface. Typical output data from the code consisted of atom label, positions and velocities, chemical type, and nature of bonds to neighbors, all as a function of time. We took the positions of all the atoms at any instant of time and used data explorer and IBMs Power Visualization System (PVS) to make 'three dimensional' pictures and movies of the deposition. Examples are shown in the Figures 1 to 4 for films of pure carbon deposited at energies between 1 and 100 eV. Carbon atoms are incident from the top. The regular array of an 8x8 diamond lattice is partially visible at the bottom of each figure. On top of the diamond substrate in the amorphous film all sorts of chemical structures are visible, in some pictures graphite-like layers are visible whilst others have 'dangling' chains of carbon. Video movies made with the PVS were particularly helpful in understanding the dy-

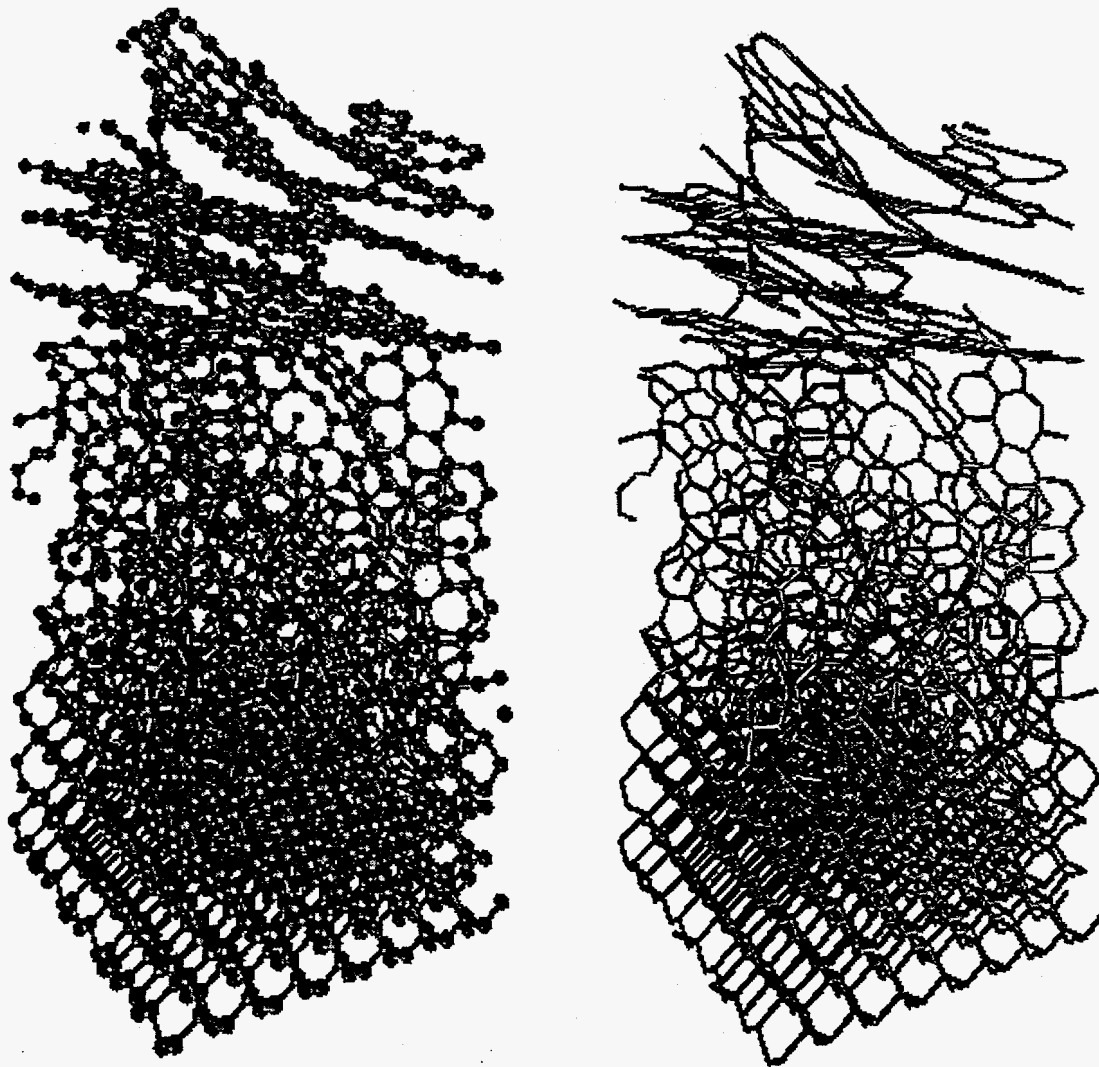


Figure 1. Perspective plot of an amorphous film of pure carbon growing on top of a diamond substrate. Left shows atoms and bonds, right shows bonds only. The 8x8 diamond substrate is seen on the bottom. Carbon atoms were incident on the substrate at an energy of 1 eV. Note the apparent low density of the film with dominant sp^2 bonding and partial graphitic structures, including well developed layers on the surface.

namics of the growing surface. On the (100) diamond surface, precursors to growth appeared to be transient snake-like chains of carbon atoms.

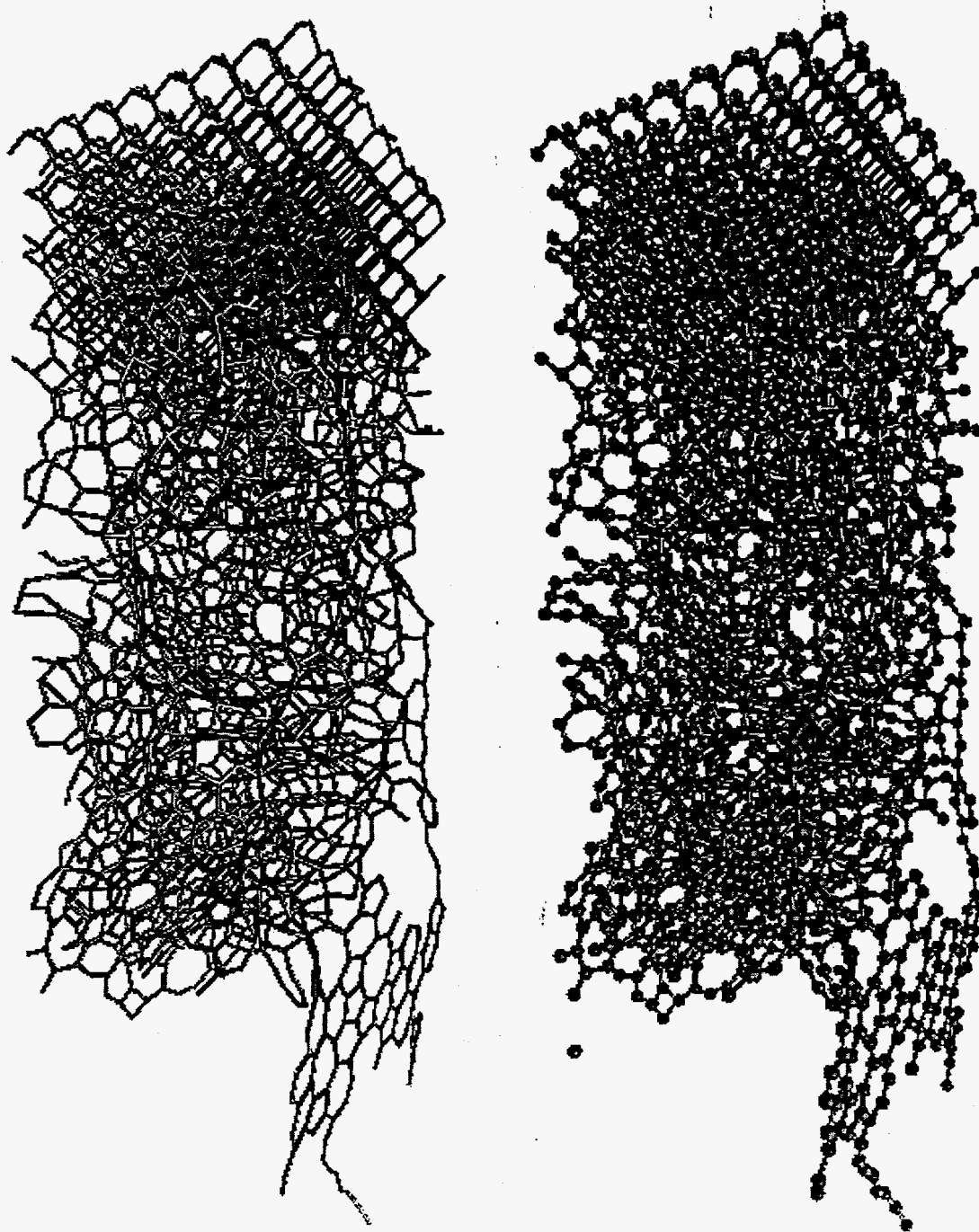
Carbon atoms travelling normal to the surface with fixed energies in the range 1 to 100 eV impinged at random (x,y) positions at the rate of 1 atom/ps. Faster deposition rates did not allow the thermostat enough time to remove the heat of reaction as the incident atom formed new chemical bonds at the surface. Experimental deposition rates are equivalent to 2 or 3 atomic layers per second, which is about 10^{10} times slower than in this theoretical simulation. The computer simulation was open, any molecular fragment that formed in the vapor phase above the surface or broke loose as a result of atom impact, and migrated past the upper boundary of the simulation cell, were removed from the simulation. This meant that the time to grow a film to a given thickness was unknown at the start of a calculation. Since the periodicity of the simulation cell in the xy plane was about 2 nm, it can be seen that the films are between 4 and 6 nm thick. Figures 1 through 4 show snap shots of a:C films growing with C atoms incident at energies of 1 eV, 5 eV, 20 eV and 50 eV respectively. In each of these figures the left hand side shows atoms and bonds and the right hand side bonds only. Time lapsed in these calculation was a few nanoseconds. The microstructure and surface morphology of the films changes strongly with incident energy.

The film in Figure 1 was grown at 1 eV. The diamond substrate is mostly intact since only the two top layers of the diamond lattice were significantly altered by reaction with the incident carbon atoms. Most of the deposited atoms are in the sp^2 state and the bonds are mostly trigonal. The film has two regions, the part next to diamond appears loose and fluffy, the part on top is graphitic. The presence of graphite may be due to the small size of the simulation cell which favors planar structures once they have nucleated and grown in size comparable to the cell size. The low overall density is evident from the apparent openness of the structure compared to the films grown at 20 eV and 50 eV.

The film in Figure 2 was grown at 5 eV. Figure 5 shows the calculated number densities for all C atoms, and those in sp^1 , sp^2 , and sp^3 state. This film is more dense there being no extended graphitic structures except for one extending vertically from the surface. We interpret the lack of planar graphite regions as an effect due to energetic atoms that pound away at the surface thereby limiting the size of planar graphitic regions. Though most of the atoms are in the sp^2 state, there is a significant concentration of sp^3 throughout the film, and also a smaller but significant concentration of sp^1 atoms.

The film in Figure 3 was grown at 20 eV. Figure 6 shows the calculated number densities for all C atoms, and those in sp^1 , sp^2 , and sp^3 states. This film is more dense than the 5 eV film, the ring structures tend to be small. The energetic atoms not only pound the surface but also penetrate further. Implanting a C atom into a sp^2 network will result in the formation of some sp^3 atoms. In this film, see Figure 6, sp^3 is the dominant hybridization of the C atom. There is a significant concentration of sp^3 across the film, also a small sp^2 which peaks near the surface. The sp^1 C atoms are concentrated at the surface.

Figure 2. Perspective plots of amorphous film of pure carbon growing on top of a diamond substrate. Left shows atoms and bonds, right shows bonds only. The 8x8 diamond substrate is seen on the bottom. Carbon atoms incident at energy 5 eV. Note the low density of the film predominantly sp^2 bonding and a few partial graphitic structures oriented perpendicularly to the surface. Density higher than at 1 eV.



The film in Figure 4 was grown at 50 eV. This film is definitely more dense and there are no graphitic structures. Erosion of the diamond substrate was more pronounced than at the lower energies. The interface is not so sharp and at the surface the ratio of sp^2 to sp^1 is unity. There are few sp^3 bonds at the surface even though it is the dominant interior species. At the higher energies (we have examined 50 eV and 100 eV) a new process appears. The interior of the film is still dense but the surface is not so sharp. This appears to be due to a physical sputtering process. Each arriving atom deposits enough energy to sunder existing surface bonds and occasionally detach fragments. In passing we note that at high energies the careful attention must be given to the ability of the thermostat to conduct away the heat of reaction and on the adequacy of high energy repulsion part of the atom-atom potentials.

AMORPHOUS a:CH FILMS

Deposition simulations have been performed for a:CH films grown with a 1:1 ratio of C to H atoms. The incident H and C atoms have the same energy. The composition of the grown a:CH film was depleted in H. Generally they contained only 20 - 30 atomic percent of H. The rest of the hydrogen atoms left the system through the vapor phase in small hydrocarbon fragments. At low energy the presence of hydrogen in the films increased the number of tetrahedrally bonded C atoms sp^3 so that the ratio of sp^3 to sp^2 was higher. Another effect was to sharpen the interface in low energy films. There is also evidence from preliminary calculations that the stress in a:CH films was lower compared to a:C films built at the same energy³.

TRIBOLOGY

Space does not permit a full description of either the indentation or sliding simulations. The 2x2 nm a:C films described above were used to construct substrates for growing larger films. The procedure was first to replicate a 4x4 nm film from a 2x2 array of 2 nm sized films. The atoms in the top 2 nm of this replicated film were then used as the base for a larger sized simulation in which atoms rained down at random on the 4x4 nm substrate. As in the simulations with (100) diamond substrates all memory of the base was lost in a few layers of carbon. The indentation experiments consisted of impacting a rigid repulsive diamond probe tip with a 10 atom blunt (100) surface and three (111) side faces into the grown 4x4 nm film. The probe was programmed to a specified depth and then retracted. The simulation was then repeated starting with exactly the same initial state of the carbon film and pushing to a greater depth. The approach and retraction speeds were 35 ms⁻¹. For very small indentations the response was nearly elastic, and the load-unload portions of the curve barely distinguishable. After penetrating approximately 0.3 to 0.5 nm into the surface the load-unload curves became distinguishable. A phenomena resembling 'tearing' with irreversible flow occurred at several stages as the indenter progressed into the material. There were large movements

of carbon atoms around the rigid tip as bonds were broken and remade. A careful analysis of the bond dynamics of these processes is underway.

In the sliding experiments the film is repetitively passed under the rigid diamond tip using a periodic boundary condition in the sliding direction. The same initial 4x4 nm film used for indentation experiments was used in two sliding simulations. The first involved high speed sliding 350 ms⁻¹ at light load. The second involved lower speed sliding 35 ms⁻¹ at higher load. After many passes at high speed the surface of the film was slowly altered. At high loads the behavior was quite different because the tip was started in a position of significant penetration into the film. In this case movement of the film created a groove in the surface.

CONCLUSIONS AND SUMMARY

The computer simulations show that films grown under different initial conditions show a graduation in composition consistent with generally known experimental findings and how the surface structure changes with impact energy. Many of the problems we have encountered analyzing the composition and structure of these films are generic to the deposition and surface processing of covalent materials, the science underlying the sputtering of organic monolayers being one such field¹⁹.

ACKNOWLEDGMENTS

The part of this work performed at LLNL was funded by the U.S. Department of Energy as part of a CRADA between the Lawrence Livermore National Laboratory and International Business Machines Research Division through Crada No. TC-297-92-C, "High Speed Tribology of the Head-Disk Interface by Computer Simulation," and also under contract number W-7405-ENG-48.

REFERENCES

- 1 M. P. Allen and D. J. Tildesley, *Computer Simulation of Liquids* (Oxford University Press, Oxford, 1989), pp. 88-90.
- 2 J. N. Glosli and G. M. McClelland, *Phys. Rev. Lett.* **70**, 1960-1963 (1993).
- 3 J. N. Glosli, J. Belak, and M. R. Philpott, *Materials Research Society. Symposium Proceedings.* (December 1994).
- 4 B. Dischler, A. Bubenzer, and P. Koidal, *Solid State Comm.* **48**, 105 - 108 (1983).
- 5 R. O. Dillon, J. A. Woollam, and V. Katkanant, *Phys. Rev. B* **29**, 3482 - 3489 (1984).
- 6 H. Tsai and D. B. Bogy, *J. Vac. Sci Technol. A* **5**, (1987).
- 7 S. M. Holl, R. D. Johnson, V. J. Novotny, J. L. Williams, C. E. Caley, M. Hoinkis, and R. E. Jones, *Materials Research Society. Symposium Proceedings.* 54-62 (Spring, 1994).
- 8 G. Comelli, J. Stöhr, C. J. Robinson, and W. Jark, *Phys. Rev. B* **38**, 7511 - 7519 (1988).
- 9 J. S. Li and J. S. Lannin, *Phys. Rev. Lett.* **65**, 1905 - 1908 (1990).
- 10 J. P. Ryckaert, I. R. McDonald, and M. L. Klein, *Computer Simulation of Polymers* **70** - 78 (1991).

- 11 G. C. Abells, Phys. Rev. B. **31**, 6184 (1985).
- 12 J. Tersoff, Phys. Rev. Lett. **56**, 632 (1986).
- 13 J. Tersoff, Phys. Rev. B **37**, 6991 - 7000 (1988).
- 14 J. Tersoff, Phys. Rev. Lett. **61**, 2879 - 2882 (1988).
- 15 D. W. Brenner, Phys. Rev. B **42**, 9458-9471 (1990).
- 16 J. A. Harrison, D. W. Brenner, C. T. White, and R. J. Colton, Thin Solid Films **206**, 213 - 219 (1991).
- 17 D. W. Brenner, J. A. Harrison, C. T. White, and R. J. Colton, Thin Solid Films **206**, 220 - 223 (1991).
- 18 D. A. Drabold, P. A. Feders, and P. Stumm, Phys. Rev. B **49**, 16415 -16422 (1994).
- 19 R. S. Taylor and B. J. Garrison, J. Amer. Chem. Soc. preprint (1994).

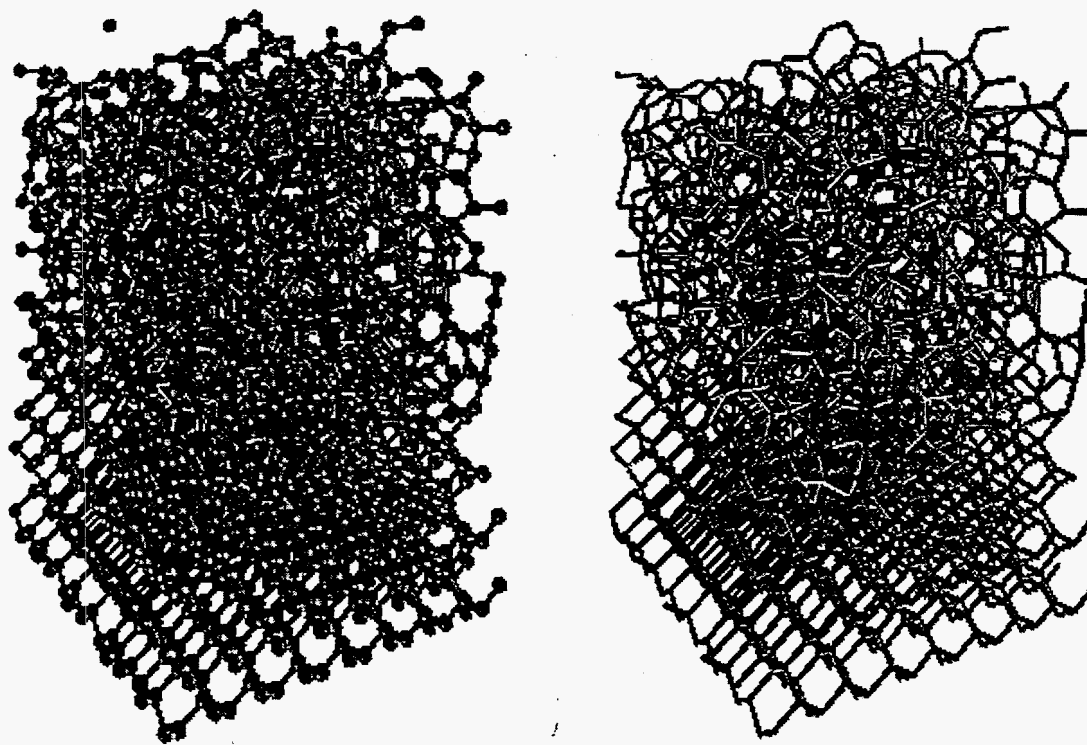


Figure 3. Perspective plots of amorphous film of pure carbon growing on top of a diamond substrate. Left shows atoms and bonds, right shows bonds only. The 8x8 diamond substrate is seen on the bottom. Carbon atoms incident at energy 20 eV. Note the higher density of the film still predominantly sp^2 bonding. There are no extended graphitic structures at the surface. Density higher than at 5 eV.

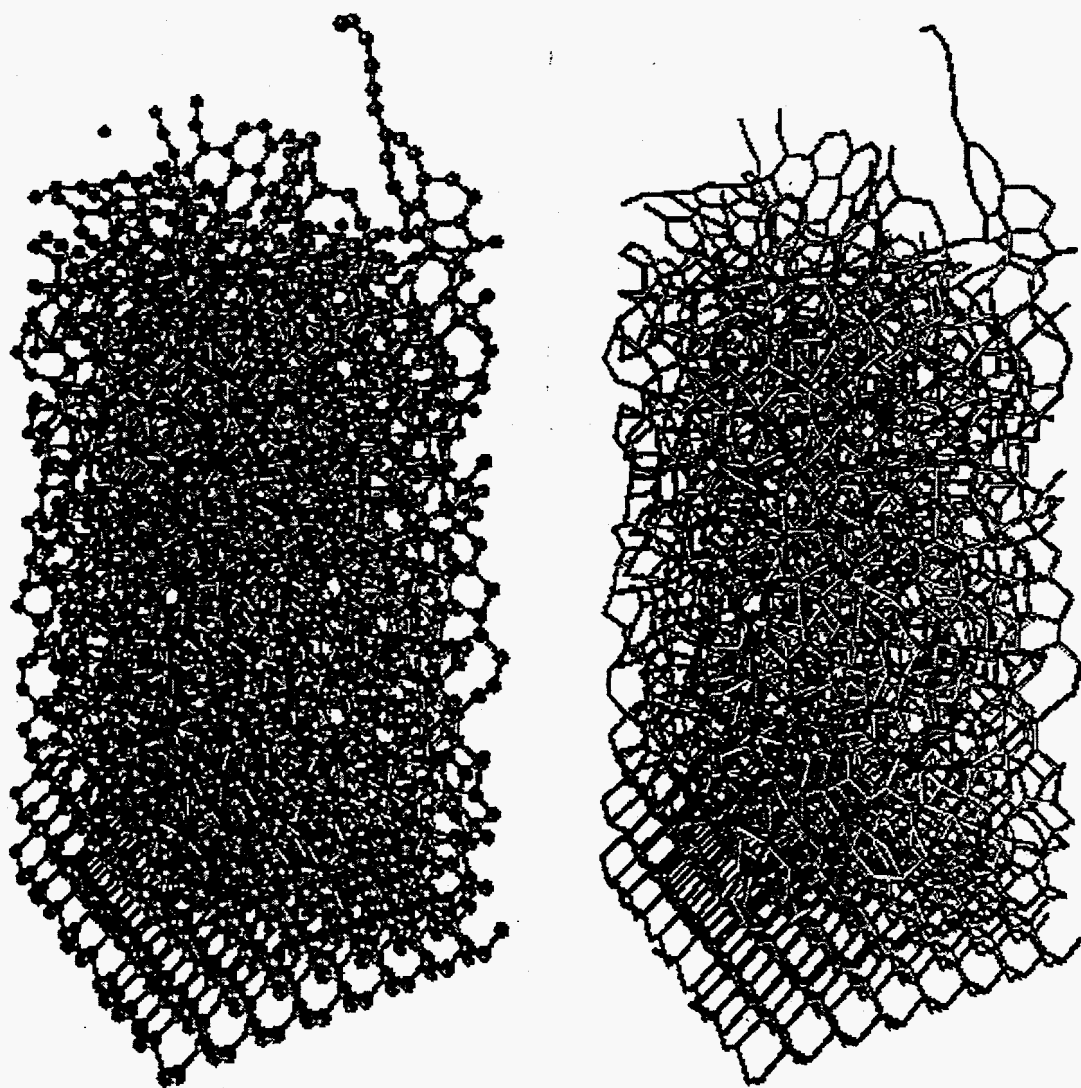


Figure 4. Perspective plots of amorphous film of pure carbon growing on top of a diamond substrate. Left shows atoms and bonds, right shows bonds only. The 8x8 diamond substrate is seen on the bottom. Carbon atoms incident at energy 50 eV. Note the higher density of the film still predominantly sp^2 bonding. There are no extended graphitic structures at the surface. Density higher than at 20 eV.

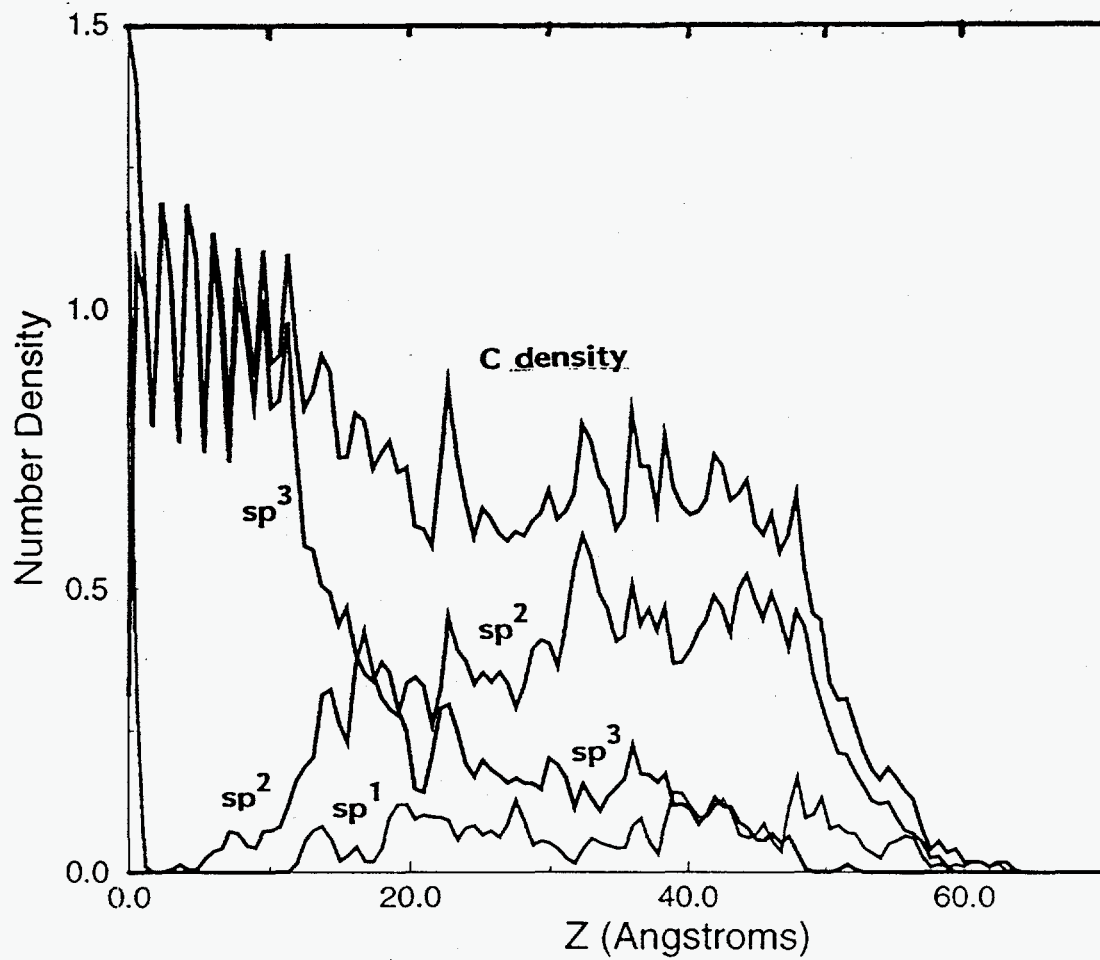


Figure 5. Density plots for an amorphous film of pure carbon deposited at 5 eV and shown in Figure 2. Note that most of the C atoms in the grown film are sp^2 hybridized. The sp^3 density drops off roughly monotonically. The sp^1 density is approximately constant across the film.

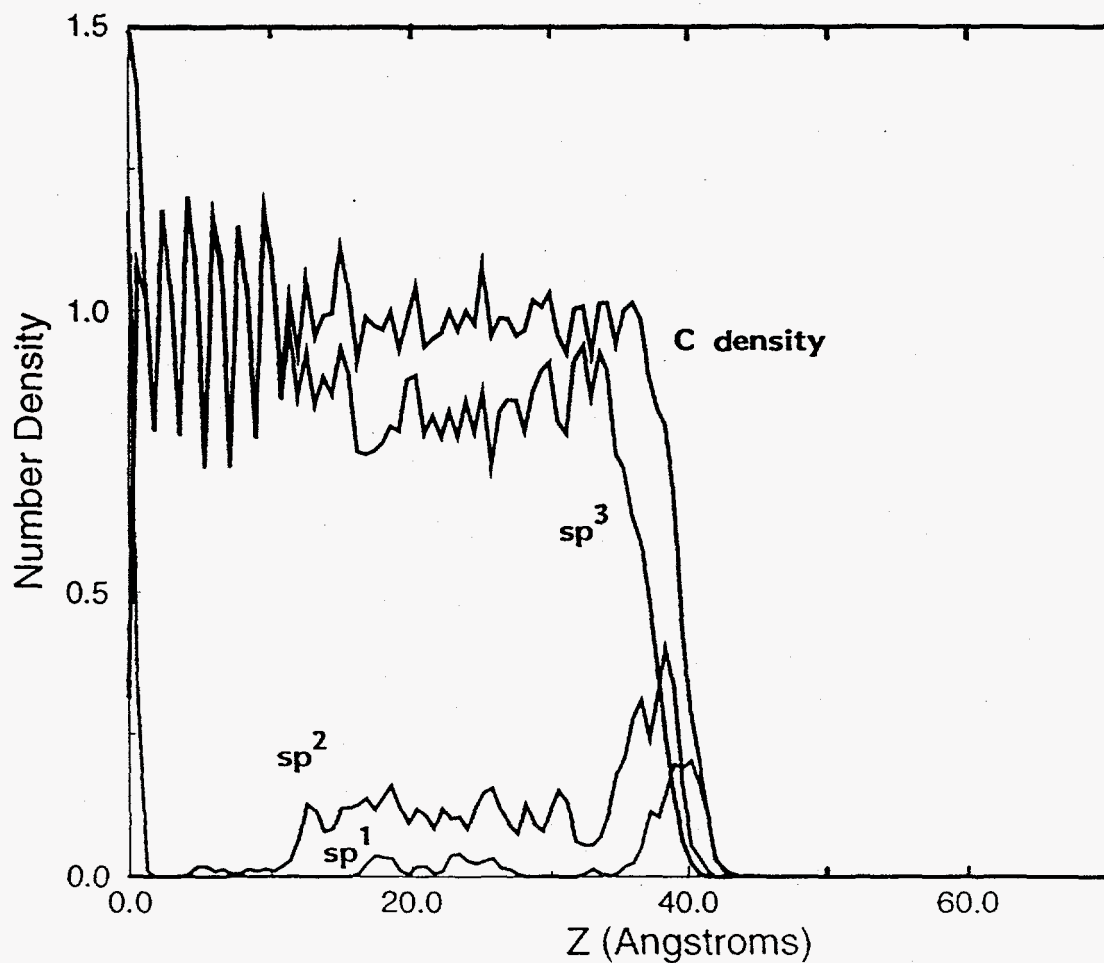


Figure 6. Density plots for an amorphous film of pure carbon deposited at 20 eV and shown in Figure 3. Note that most of the C atoms in the grown film are sp^3 hybridized. The sp^2 density is approximately constant across the film with a peak at the growing surface. The sp^1 density follows the sp^2 density but at a lower value.